Automotive Science and Engineering, Vol. 15, No. 2, (2025), 4689-4703

Iran University of Science and Technology

Automotive Science and Engineering

Journal Homepage: ase.iust.ac.ir

ISSN: 2008-9899

New approaches in driveline shunt and shuffle control by a dry clutch

Milad Badrikouhi[1*], Behrooz Mashadi[2]

[1]School of Automotive Engineering, Iran University of Science and Technology, Tehran, Iran

[2] School of Automotive Engineering, Iran University of Science and Technology, Tehran, Iran

ARTICLE INFO

Article history:

Received: 25 Oct 2024

Accepted: 15 Apr 2025

Published: 2 May 2025

Keywords:

Shuffle

Shunt

Driveline modeling

Clutch abrasion control

Driveline oscillation

ABSTRACT

A new idea is applied for damping of driveline oscillation (shunt and shuffle) created because of sudden changes in transmitting engine torque. In this case, by an actuator the dry clutch slides due to decreasing in clutch clamp force. By regulating the clutch force, it prevents the excessive torque from entering the driveline, which causes vibrations. This strategy eliminates the oscillations. Hence, the driveline dynamics which consists of the clutch model, driveline elements, backlash, and tire slip is modeled comprehensively in the MATLAB software and validated. When the vibrations are sensed by sensors, the electronic control unit directs the clutch actuator by changing the normal clutch force so the dry clutch slides and dampens the vibrations. For this idea, three controlling approaches are suggested: a rule-based controller, a pulse controller, and a linear predictive controller. Essential tests for examining driveline control performance are chosen and then the driveline performance is assayed for it. Also, one of the priorities in selecting a clutch control strategy is to increase the clutch lifetime. From the results, driveline vibrations including shunt and the shuffle can be reduced well. In addition, this idea doesn't have the harms of the other solutions such as spark advance engine control that pollutes the air and electronic throttle control which lessens the vehicle performance. Moreover, the usage of this system is simple, especially in vehicles that have automatic manual transmission.

1. Introduction

Historically, NVH (noise, vibration, and harshness) has been an important problem for automakers [1, 2]. The main sources of NVH are wheels, engine, and driveline system. Unwanted vibrations cause great harm to automobiles for example failure of some components due to fatigue, component failure such as rubber coating, vibration and noise in a car, and lack of comfort and drivability. Avoiding these cases is vital in the commercial success of a product.

Drivability is a collection of factors regarding driving comfort [3, 4]. Drivability is the sensation of a driver within driving conditions. On the other hand, the driveline is one of the sources of vibrations [5]. Through transient situations for example gearshifting, tip-out, tip-in, and falling in bump, backlash traverse and elastic elements (driveshaft and transmission shaft) cause unwanted vibrations. By these, various kinds of vibrations are created such as shunt, shuffle, clunk, judder, rattle, and clatter [6]. These vibrations via driveline transfer to the automobile which cause vehicle longitudinal vibrations. Thus, passenger comfort and drivability are destroyed. Moreover, the oscillations diminish the durability of elements by reason of high mechanical contact stress [7].

*Corresponding Author
Email Address: miladbadrykoohi@yahoo.com
https://doi.org/10.22068/ase.2025.696

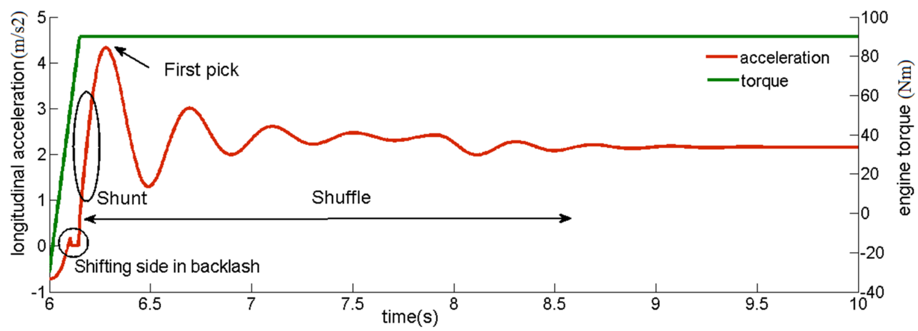

Figure 1: Shuffle and shunt vibration.

This paper concentrates on shunt and shuffle, two cases of driveline vibrations [8, 9]. They are experienced as a keen jerk (shunt) which is pursued by a continuation vibration (shuffle). These phenomena (Figure 1) happen with quick fluctuations in transmitted torque to the driveline. Plus, the gear ratio can affect the amplitude of the vibrations. The shuffle and shunt phenomenon depend on the value of vehicle parameters. Ordinary in passenger cars, these happen in 1-10 Hz frequency. Unfortunately, the resonance frequency of the human body is in the same range [10], for instance, shoulder resonance frequency is 4-6 Hz, stomach resonance is in the frequency of 4-8 Hz, and upper body resonance is between 3-6 Hz. So with these facts, those vibrations must be controlled [11].

Until now, for attenuating these vibrations, various probes and methods have been performed. It is necessary to detect how the torsional stiffness of the driveline elements affects driveline torsional modes [12]. In the other research, isolation of engine firing oscillation from the driveline is the operative method to decrease rattle vibration. Torque profile shaping is another way that diminishes shock and jerk [13]. Spark advance engine control is the method in which the controller utilizes the engine to control the driveline vibrations [14-16]. Controlling by changing the ratio of air-fuel is the method for reducing the vibrations. When more or less torque is demanded, the controller tunes the torque by decreasing or increasing fuel in the blend of air-fuel [17]. In other research, an electric motor has been used to dampen the vibrations in hybrid vehicles [18-20]. Further, by controlling the electronic gas pedal, abrupt variations in transferred torque to the driveline have diminished [21].

But the procedures mentioned above have some bugs. Electric motors for controlling vibrations are only utilized in hybrid vehicles, therefore it has no general use. Varying in the driver torque demand in the electronic gas pedal control and controlling by changing the ratio of air-fuel, lead to reducing automobile performance. Changing the spark engine timing in spark advance engine control causes disarrange the combustion settings and this subject leads to polluting the air. In addition, a limitation is existed in generating the torque that the controller needs, because the engine may not be able to generate it. Also, totally, in some papers some parameters for example tire slip [21] and backlash traverse [22], have been omitted in modeling.

As a solution for these cases, a new approach is surveyed in this paper. The idea is to use a dry clutch as an actuator similar to the half-clutch technique. In this way, by an actuator, the normal force in a dry clutch is adjusted so the two faces slide to each other and the extra vibration torque converts to heat and wastes. This method has simple applications, particularly in automobiles that have automated manual transmission (AMT) gearbox systems [22, 23]. The idea of using a clutch to dampen the vibrations is shown in Figure 2. When the flywheel torque, T_f is increased abruptly and excessively, the clamping force of the clutch is reduced to eliminate the excess torque that causes vibrations. T_c is the clutch torque that enters the driveline.

In comparison with the previous work of the authors of this article [24], three different strategies for dry clutch control are introduced and then compared in this work. In addition to that, using the clutch control as an actuator for controlling driveline oscillations has been examined in 2nd gear ratio this time. Also, backlash modeling has become more complete in this work. Moreover, one of the priorities in choosing the control strategy in this article is to focus on increasing the clutch lifetime. Thus, the main contributions of this research are:

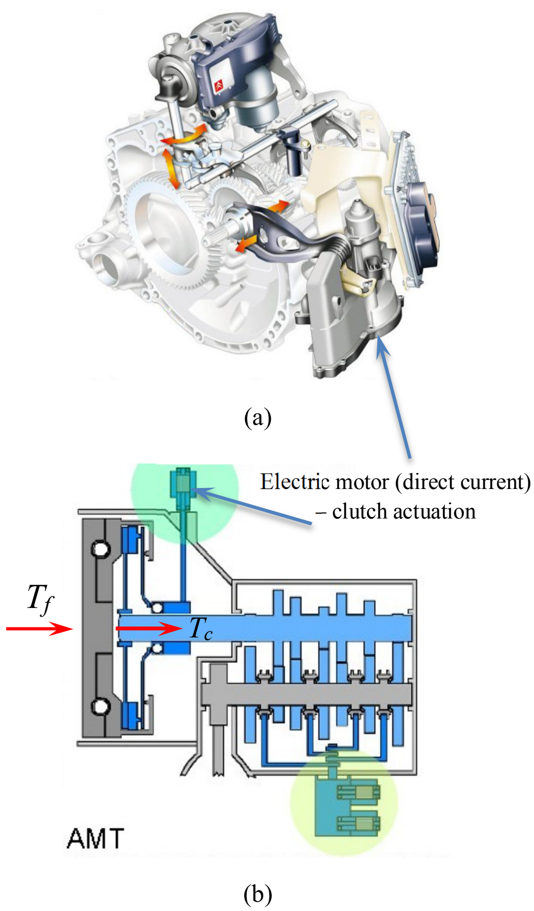

Figure 2: AMT transmission. (a): AMT schematic model, and (b): AMT gearbox actuators.

(1) The idea of using a dry clutch to control the vehicle's longitudinal vibrations is investigated. By adjusting the normal force of the clutch, the torque passing through the transmission line is adjusted and the vibrations are prevented.

(2) Three types of controllers based on normal clutch force control are discussed. In addition to the performance of controllers in controlling vibrations, clutch wear is also checked.

(3) To examine the controller's performance, a comprehensive model of the transmission line, including a modified backlash model, clutch, and a complete tire model, is presented.

In this research in Section 2, the driveline will be modeled. In Section 3, the controllers are designed, and the tip-in scenario for testing driveline vibration is introduced and the responses of the controller are surveyed. Finally, the gain scheduling controller is argued and the results are displayed in Section 4 before the conclusion section. With clutch control idea with low-cost implementation, it can achieve good drivability moreover it can avoid polluting the air and diminishing vehicle performance.

2. Vehicle driveline modeling

Before the controllers are designed, first the driveline must be modeled. The driveline model is a high-order model with nonlinearities [25] which is expressed in the following sections. The parameters in vehicle modeling are represented in Table 1.

Table 1: Nomenclatures

Name	Symbol	Unit
Torque	T	Nm
Velocity	v	m/s
force	F	N
Overall gear ratio	n	-
Stiffness coefficient	k	Nm/rad
Car frontal area	A	m^2
Damping coefficient	b	Nm.s/rad
radius	r	m
Road gradient	β	Rad
Backlash angle	2α	Rad
angle	θ	Rad
Rolling resistance coefficient	f_R	_
Drag coefficient	C_d	_
Inertia	I	Kg.m^2
Angular velocity	ω	Rad/s
Gravitational acceleration	g	m/s^2
Vehicle mass	m	kg
Air density	ρ	Kg/m^3
Friction coefficient	μ	_
Slip	s	_

2.1. Clutch system modeling

The clutch is the part of the driveline that links the engine to the wheels. A dry clutch involves two or various plates, which are clamped to each other by a spring. In the simple model of Figure 3 a clutch with a single surface is shown. The clutch has two kinds of plates: The friction plate and the pressure plate. The pressure plate is assembled on the flywheel by bolts and receives engine torque. The friction plate transmitted the torque to the gearbox. The driver can disconnect these two plates by a normal force acting on clutch springs. If the clutch has an actuator, it can arrange the normal force F_n. If F_n is reduced, the friction plate slips and the oscillation torque does not pass and converts to heat, hence by tuning F_n, the oscillations can be dampened. In Figure 3, the clutch torque is T_{cl}, T_e deputes the engine torque, the load torque from the driveline is T_d, the friction coefficient of the clutch is μ, and ω_e is the engine angular velocity.

Choosing a model for the friction coefficient of a clutch μ is important. In some papers, the modeling of a driveline was considered very simple. For example clutch model is a combination of static and kinetic friction [26], the coulomb friction model, and the stick-slip friction model [27]. On the other hand, detailed modeling for the friction coefficient of a clutch face is necessary so there are acceptable models for friction such as the neural network model [28], the hybrid model, and the lugre model for dry friction [29].

For this article for modeling of friction coefficient reset integrator model is chosen. The reset integrator model is based on the bristle model [30]. The bristle model explains the friction of a surface in the microscopic form. Indeed, the surface is not smooth and has many disordered points. This contact point is presumed as a bristle. If two surfaces move toward each other, the contact among these bristles grows and friction increases to the high stage of static friction. The friction force is explained as follows:

$$F_{fric} = \sum_{i=1}^{m} \sigma_0 \left(x_i - b_i \right) \qquad (1)$$

Where m is the number of bristles, σ_0 is the stiffness of each bristle, and can be a function of velocity and $(x_i\text{-}b_i)$, the relative displacement in bristles. (Figure 4)

However, this model is computationally useless; consequently, it is not efficient in simulation. So, the reset integrator model for simulation that considers the stribeck effect is expressed by Haessig and Friedland [30]. A characteristic of this model is a region named a dead zone or stiction zone. The friction force in this zone depends on relative displacement, x_{rel}, and velocity, v_{rel}. It is computed from (2).

$$F_{fric} = K_{stick} x_{rel} + B_{stick} v_{rel} \qquad (2)$$

where K is the stiffness coefficient and the damping coefficient is B. After the relative displacement reaches the threshold dx, the friction is calculated in the sliding zone. In the sliding zone, the friction force is represented as (3) that depends on the stribeck effect and viscous friction:

$$F_{fric} = f_{slip} + (f_{stick} - f_{slip}) e^{\left(\frac{-3|v_{rel}|}{astrib}\right)} + f_v v_{rel} \qquad (3)$$

In Figure 5, f_{stick}, f_{slip}, v_{rel}, *astrib*, and f_v are stiction friction, coulomb friction; relative velocity, stribeck constant, and viscous damping coefficient. Thus, the friction model includes linear and nonlinear parts.

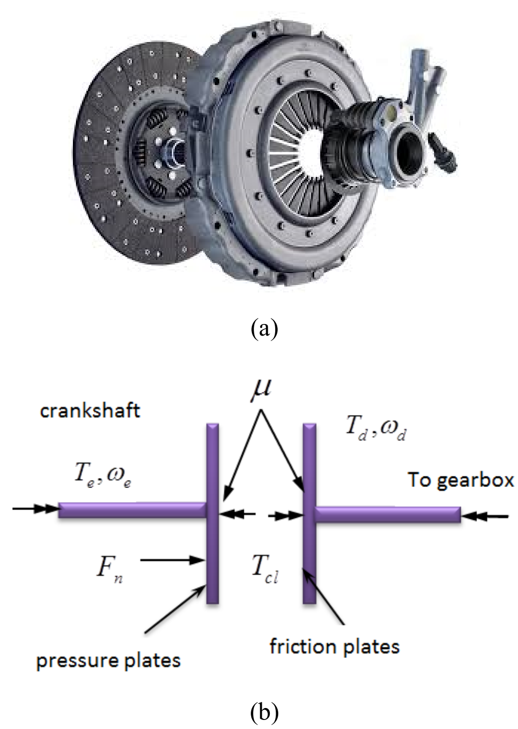

Figure 3: Clutch model. (a): A dry clutch, and (b): free body diagram (FBD) of a clutch.

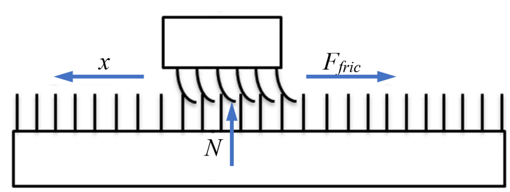

Figure 4: Bristle model for friction.

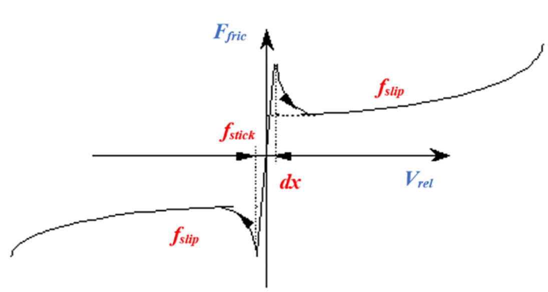

Figure 5: Friction modeling versus relative velocity.

In Table 2, these parameters are expressed.

Table 2: The friction model parameters.

Name	Abbreviations	Value
Velocity	v_{rel}	-
Viscous damping coefficient	f_v	0
Coulomb friction	f_{slip}	0.24
Stiction friction	f_{stick}	0.30
Stribeck constant	*astrib*	600

Moreover, the friction plate consists of torsional springs arranged around a driven hub (Figure 3a). The stiffness of these springs determines how the torque is transmitted from the flywheel to the driveline. As shown in Figure 6 clutch torsional stiffness coefficient is k_{c1} for the angle from 0 to θ_{c1}, and k_{c2} for the angle from θ_{c1} to the end mechanical stop, θ_{c2}. The torque due to the clutch torsional stiffness can be designated as follows:

$$\theta_c = \theta_f - n\theta_t \tag{4}$$

$$T_{ck} = \begin{cases} k_{c1}\theta_c & \text{If } \ |\theta_c| \le |\theta_{c1}| \\ k_{c1}\theta_{c1} + k_{c2}(\theta_c - \theta_{c1}) & \text{If } \ |\theta_{c1}| \le |\theta_c| \le |\theta_{c2}| \\ k_{c1}\theta_{c1} + k_{c2}(\theta_{c2} - \theta_{c1}) & \text{If } \ |\theta_c| \ge |\theta_{c2}| \end{cases} \tag{5}$$

Also, the clutch damping coefficient is c_c. Thus, the clutch torque due to damping is $T_{cc} = c_c\dot{\theta}_c$. Consequently, the overall clutch torque T_c which transmits to the gearbox can be written as $T_c = T_{ck} + T_{cc}$

2.2. Driveline

The modeling of the driveline which includes its main parts is displayed in Figure 7. T_c, T_f, T_d, and T_t signify the clutch torque, engine torque, differential torque, and traction torque equals to r_wF_t. I_f denotes the inertia of the engine plus flywheel, I_t is the inertia of the transmission and I_w represents the inertia of the wheel. θ_f, θ_c, θ_t and θ_w are angular displacements of the engine, clutch, transmission, and wheel. In addition, the overall gear ratio between the engine and wheels is considered as n (The overall gear ratio is the gearbox ratio multiplied by the final drive ratio).

$$I_f\ddot{\theta}_f = T_f - T_c \tag{6}$$

$$I_t\ddot{\theta}_t = nT_c - b_t\dot{\theta}_t - T_d \tag{7}$$

where the transmission damping is b_t, and T_d is the driveshaft torque. Also, the dynamics of the wheel is defined as:

$$I_w\ddot{\theta}_w = \frac{T_d}{2} - r_w\frac{F_t}{2} \tag{8}$$

The traction force is F_t which depends on the normal force of a tire, F_z, and slip, s.

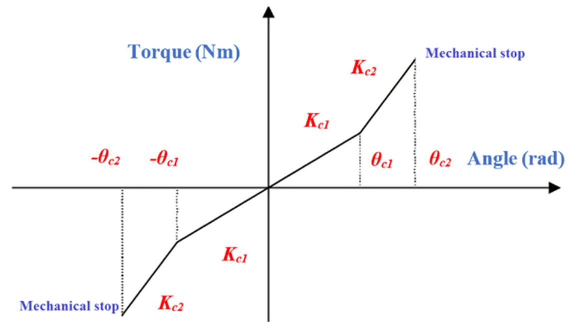

Figure 6: Clutch stiffness coefficient [21].

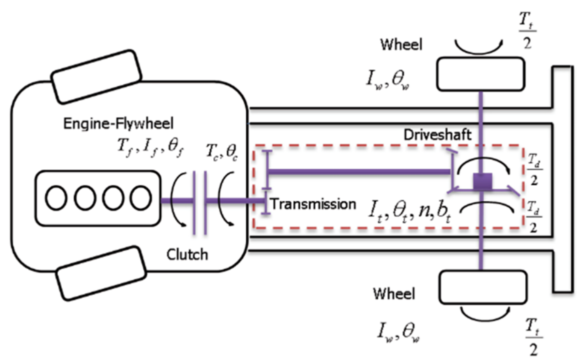

Figure 7: Vehicle driveline modeling.

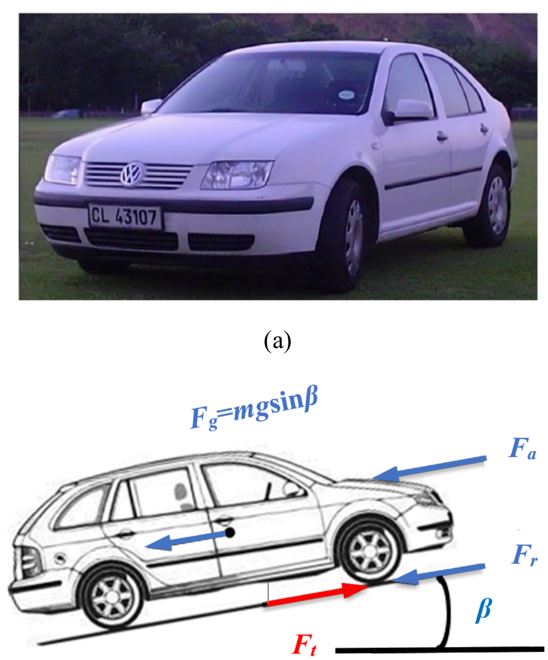

(a)

(b)

Figure 8: Vehicle model. (a): Volkswagen Jetta [21] and (b): FBD of a Volkswagen Jetta.

Vehicle motion depends on the driveline and wheel dynamics and tractive and resistive forces. From the FBD of the vehicle in Figure 8, the equation of motion is written as:

$$m\dot{v} = F_t - F_a - F_r - mg\sin\beta \tag{9}$$

where F_r is the rolling resistance force and F_a is the aerodynamic force.

$$F_a = \frac{1}{2}C_d A\rho v^2 \tag{10}$$

$$F_r = f_R mg \tag{11}$$

A, C_d, ρ, f_R, v, β, and m are respectively the car's frontal area, the drag coefficient, the density of the air, the rolling resistance coefficient, car velocity, the gradient of the road, and the mass of the vehicle.

2.3. Backlash modeling

Backlash is clearance among driveline components and is one of the important factors that cause unpleasant vibrations (Figure 9). The backlash is an intensive nonlinear phenomenon. The backlash zone is the region where the engine torque does not transfer to the wheels and there is no contact between two parts of the driveline but when the two parts adjoin together again, the torque transmits into the driveline abruptly. The lash between gears in the gearbox as clearances is the source of backlash that is required to gearbox works in high temperatures (Figure 9). The existence of backlash is essential in producing gears so this case usually occurs in the gearshifting process in the gearbox and differential. The angle of the backlash is greater; the intensity of oscillations is harsher. Various models for backlash traverse have existed. In this research, one of the best, the modified dead zone model is utilized.

The formulation that represents this phenomenon is:

$$\theta_{rel} = \theta_t - \theta_w \tag{12}$$

$$T_{dz} = \begin{cases} k_s(\theta_{rel} - \alpha) + c_s\dot{\theta}_{rel} & \text{If} \quad \theta_{rel} > \alpha \\ k_s(\theta_{rel} - \alpha) + c_s\dot{\theta}_{rel} & \text{If} \quad \theta_{rel} < \alpha \\ 0 & \text{If} \quad |\theta_{rel}| \le \alpha \end{cases} \tag{13}$$

$$T_d = \begin{cases} 0 \quad \text{If} \begin{bmatrix} T_{dz} < 0 \text{ and } \theta_{rel} > 0 \\ T_{dz} > 0 \text{ and } \theta_{rel} < 0 \end{bmatrix} \\ T_{dz} \quad \text{Otherwise} \end{cases} \tag{14}$$

where c_s and k_s are the shaft damping and stiffness. θ_{rel} is the relative angle between two parts of the shaft and α is the backlash angle.

2.4. Slip

A perfect tire longitudinal force model which depends on the slip and tire normal force is considered in driveline modeling. The slip definition is represented in (15):

$$s = \begin{cases} 1 - \dfrac{r\omega}{v} & \text{If} \quad v > r\omega \\ 1 - \dfrac{v}{r\omega} & \text{If} \quad r\omega > v \end{cases} \tag{15}$$

where the radius of the tire is r, the angular velocity of the tire is ω and the car velocity is v. The Pacejka model is selected for this paper. This model is the most well-known and practical model for the tire longitudinal force. In the Pacejka tire model, longitudinal force depends on normal force and the tire slip. The model is explained in [31].

$$F_t = F(s, F_z) \tag{16}$$

2.5. Validation of the driveline modeling

To research the performance of controllers in the test condition, an accurate model is required. The model of this work is validated with the experimental data in [21] (Northcote thesis) which is based on a 1.6-liter Volkswagen Jetta. The parameters of the Volkswagen Jetta are presented in Table 3.

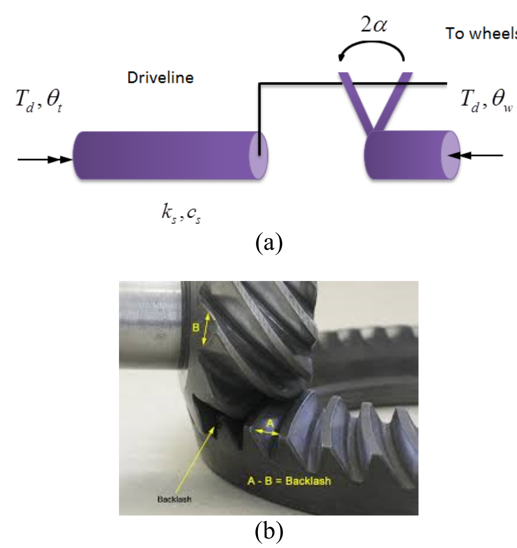

Figure 9: Backlash. (a): FBD of backlash and (b): backlash between gears as a source of vibration.

It is fitted an accelerometer to the Volkswagen Jetta to measure the longitudinal acceleration, and shunt and shuffle were induced by quickly accelerating and decelerating in second gear. The results obtained from the model of this article are compared to the measured accelerometer data obtained in the vehicle test. Before a direct comparison, the accelerometer data had to be digitally filtered.

Table 3: The parameters of the Volkswagen Jetta [21]

Name	Symbol	Unit	Value
The overall gear ratio in 2nd gear	n	-	7.65
Road Gradient	β	-	0
Rolling resistance coefficient	f_R	-	0.0136
Backlash angle	2α	rad	0.0785
Transmission inertia	I_t	kg.m^2	0.0100
Tire inertia	I_w	kg.m^2	1.0000
Flywheel inertia	I_f	kg.m^2	0.1700
Drag coefficient	C_d	-	0.3000
Tire radius	r_w	m	0.3200
Clutch stiffness (0 – 0.2094 rad)	k_{c1}	Nm/rad	854
Clutch stiffness (0.2094 – 0.2443 rad)	k_{c2}	Nm/rad	1672
Car frontal area	A	m^2	2.2000
Vehicle mass	m	kg	1400
Drivetrain damping coefficient	c_s	Nm.s/rad	90
Driveshaft stiffness coefficient	k_s	Nm/rad	6420

Figure 10 compares the simulation and experimental data for a ramp in engine torque in the first second from -40 Nm to 130 Nm in 0.15 seconds. A near similarity that is observed validates the modeling accuracy of this paper. Also, this model can predict the shunt and shuffle in the drivetrain very well [21].

2.6. Simplified model of the driveline

To estimate the desired acceleration that a driver demands, it is necessary to choose a simplified linear model that has the main characteristics of a high-ordered model. This simplified model is used by Fredriksson[14] and Northcote[21], too. This model involves the engine-flywheel inertia and wheel inertia which is linked together with a torsional spring and a torsional damper. The spring and damper represent the driveshaft elasticity and damping coefficient. In this model, some nonlinear effects for example the engine dynamic, frictional effect of driveline, backlash traverse, and tire slip are neglected. Also, some inertia for example the transmission inertia is ignored because it is too small rather than flywheel inertia. Another notice is that the clutch is engaged (Figure 11). Therefore, the equation of motion is rewritten as follows:

$$I_f\ddot{\theta}_f = T_f - T_c \tag{17}$$

$$nT_c = T_d \tag{18}$$

$$\theta_f = n\theta_d \tag{19}$$

$$T_d = k_s(\theta_d - \theta_w) + c_s(\dot{\theta}_d - \dot{\theta}_w) \tag{20}$$

$$2I_w\ddot{\theta}_w = T_d - r_w F_t \tag{21}$$

$$v = r_w\dot{\theta}_w \tag{22}$$

$$m\dot{v} = F_t - F_a - F_r - mg\sin\beta \tag{23}$$

By simplification of (17)-(23), it is resulted that:

$$I_f\ddot{\theta}_f = T_f - \frac{T_d}{n} \tag{24}$$

$$T_d = k_s\left(\frac{\theta_f}{n} - \theta_w\right) + c_s\left(\frac{\dot{\theta}_f}{n} - \dot{\theta}_w\right) \tag{25}$$

$$I_f\ddot{\theta}_f = T_f - T_c \tag{26}$$

After considering:

$$I_c = 2I_w + mr_w^2 \tag{27}$$

$$T_t = (F_r + F_a + mg\sin\beta)r_w \tag{28}$$

As a result, the dynamic modeling of the simplified model (Figure 11) is as follows:

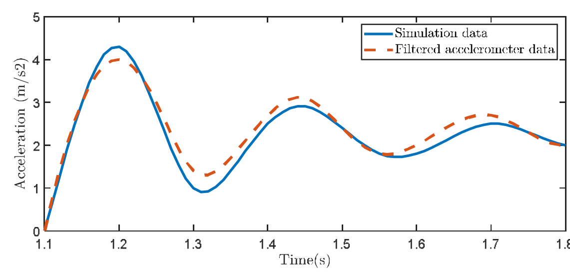

Figure 10: Validation of the model with experimental data (response to engine torque ramp: -40 Nm to 130 Nm in 0.15 seconds).

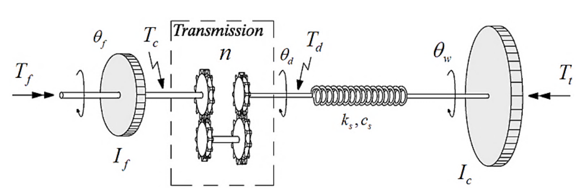

Figure 11: Simplified model for vehicle driveline [14].

$$I_f\ddot{\theta}_f = T_f - \left(\frac{k_s}{n}\left(\frac{\theta_f}{n}-\theta_w\right)+\frac{c_s}{n}\left(\frac{\dot{\theta}_f}{n}-\dot{\theta}_w\right)\right) \quad (29)$$

$$I_c\ddot{\theta}_w = k_s\cdot\left(\frac{\theta_f}{n}-\theta_w\right)+c_s\left(\frac{\dot{\theta}_f}{n}-\dot{\theta}_w\right)-T_t \quad (30)$$

The state space form of the equations is:

$$\begin{bmatrix}\dot{X}_1\\ \dot{X}_2\\ \dot{X}_3\end{bmatrix}=\begin{bmatrix}0 & -1 & \frac{1}{n}\\ \frac{k_s}{I_c} & -\frac{c_s}{I_c} & \frac{c_s}{nI_c}\\ -\frac{k_s}{nI_f} & \frac{c_s}{nI_f} & -\frac{c_s}{n^2I_f}\end{bmatrix}\begin{bmatrix}X_1\\ X_2\\ X_3\end{bmatrix}+\begin{bmatrix}0 & 0\\ 0 & -\frac{1}{I_c}\\ \frac{1}{I_f} & 0\end{bmatrix}\begin{bmatrix}T_f\\ T_t\end{bmatrix} \quad (31)$$

where:

$$X_1=\left(\frac{\theta_f}{n}-\theta_w\right) \quad (32)$$

$$X_2=\dot{\theta}_w \quad (33)$$

$$X_3=\dot{\theta}_f \quad (34)$$

In which:

$$y=\dot{X}_2=\ddot{\theta}_w \quad (35)$$

3. Controller design

For achieving good drivability, the shunt and shuffle must be attenuated so perfect controllers must be designed. For this purpose, a reference input is needed. This input is desirable acceleration that a driver wants to eventually reach. Also, it is noticed that the shuffle and shunt phenomena depend on the gear ratio. The amplitude of these vibrations reduces in higher gears whereas the frequency of them increases. Fortunately, this approach can simply be used in every gear. In this paper, the controller design will be done for the second gear (Figure 12).

3.1. Clutch control approach

The method of clutch control is to utilize a predictable controller. The primary idea is when the shunt and shuffle are going to happen the controller diminishes the normal force of a clutch. By this, the capacity of clutch frictional torque decreases and the two sides of clutch can slide to each other. Thus, the extra torque which leads to longitudinal vibrations converts to heat.

The estimate of probable vibrations is very significant for the controller. In reality, a series of sensors like the road gradient sensor and throttle position sensor will be required. These sensors are utilized in other controlling systems like ABS, hill-start assist control, and ESP. The probability of oscillation can be detected by the throttle position sensor meanwhile the gas pedal position varies rapidly through the tip-out or tip-in; therefore, the controller starts. Also, from the gas pedal position sensor and the rate of its variations, the requested acceleration can be approximated thus, the maximum of T_c and the maximum of N_c are calculated. This normal force is actuated to clutch by the actuator:

$$N_c=\frac{T_c}{\mu_c r_c} \quad (36)$$

where r_c and μ_c are the radius of the clutch and the friction coefficient of the clutch. Consequently, the oscillation is lessened without devoting the vehicle performance.

3.2. Acceleration, torque, and clutch clamp force estimation

For computing the desired normal force that must be exerted on the clutch, the desired acceleration $\ddot{\theta}_d$ must be guesstimated. This is the desired acceleration of the driver and this acceleration happens after the transient condition. For approximating this acceleration, the state space of the simplified model from section 2.6. is used. Inserting the parameters of the Volkswagen Jetta, the transfer function between acceleration and engine torque as between acceleration and load torque can be generated as:

$$\frac{y}{T_f}=\frac{s^2\theta_w(s)}{T_f(s)}=\frac{0.4794\,s+34.2}{s^2+9.67s+689.8} \quad (37)$$

$$\frac{y}{T_t}=\frac{s^2\theta_w(s)}{T_t(s)}=-\frac{-0.006927s^2-0.06266s-4.47}{s^2+9.67s+689.8} \quad (38)$$

The steady state is gotten when time tends to infinity. This is equivalent to $s\rightarrow 0$. Therefore:

$$\frac{y}{T_f}(ss)=0.0496 \quad (39)$$

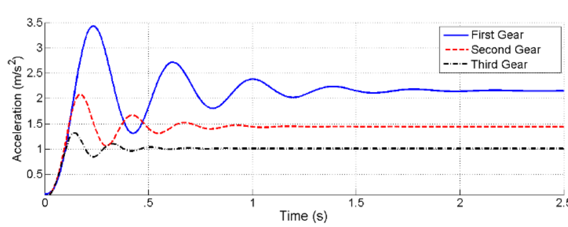

Figure 12: Vehicle acceleration. Results for the engine torque ramp 10- 90 Nm in different gears [24].

$$\frac{y}{T_t}(ss) = -0.0065 \qquad (40)$$

therefore, the requested rotational acceleration of the wheel is computed as follows:

$$\ddot{\theta}_d = u = 0.0496T_f - 0.0065T_t \qquad (41)$$

T_f depends on engine angular velocity and gas pedal, thus it can be calculated from the engine map by the data from the engine speed sensor and electronic gas pedal sensor. The load torque T_t, as represented in (41), depends on wheel speed and road gradient. By the wheel speed and road gradient sensors, the load torque is computed [32-34]. Thus, the desired acceleration is calculated.

3.3. Tip-in scenario

For researching the performance of the controllers, a tip-in scenario is supposed. In this scenario, the driver wants the vehicle to accelerate suddenly. This sudden acceleration is done by quick changes in the gas pedal position and can be figured out by the throttle position sensor. This case can be stated as a ramp in 0.1 seconds and engine torque varies from 10 to 90 Nm (Figure 13).

3.4. Rule-based controller

To design the rule-based controller, after determining the desired acceleration, the constraint of the normal force of the clutch is specified. This limitation is determined from section 3.2. If the acceleration exceeds from desired acceleration the controller decreases the clutch normal force and when it lessens the limitation, the clutch normal force is increased by the actuator. The controller limits the clamp force in a bandwidth.

$$N = \begin{cases} \text{If} \quad \ddot{\theta} > \ddot{\theta}_d \quad \text{Then} \quad N = N - 10 \\ \text{If} \quad \ddot{\theta} < \ddot{\theta}_d \quad \text{Then} \quad N = N + 10 \end{cases} \qquad (42)$$

which the normal force of the clutch is N, $\ddot{\theta}_d$ is the desired angular acceleration, and the angular acceleration is $\ddot{\theta}$. The response of the controller for the tip-in scenario in sixth seconds is illustrated in Figure 14.

3.5. Pulse controller

This controller generates a force with a specified frequency and attempts to limit the transferred torque from the clutch. This force is in the form of a pulse:

$$N = N_{ave} + N' \sin\left(\omega(t - t_0)\right) \qquad (43)$$

N_{ave} is the average of the force, N' is the pulse amplitude, the time is t, ω is the pulse frequency, and t_0 is the time that the controller acts. The response of this controller is shown in Figure 15.

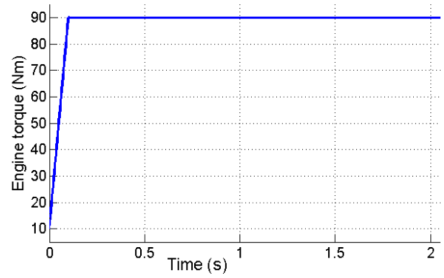

Figure 13: The engine torque, 10 - 90 Nm in 0.1 seconds.

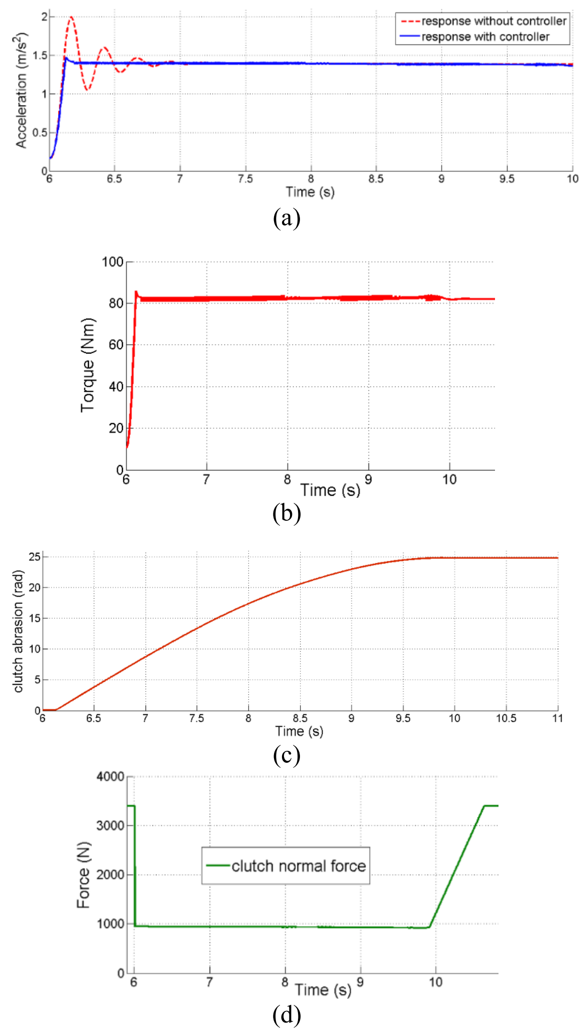

Figure 14: Vehicle response with and without the rule-based controller. (a): acceleration, (b): clutch torque, (c): abrasion between two surfaces of a clutch, and (d): clutch normal force variation.

3.6. Linear controller design

In this case, the linear controller generates the clutch's normal force and the actuator applies it to the clutch. If there is a possibility of vibration, the actuator diminishes the normal force of the clutch. This action causes the sliding of two faces of the clutch and dampens the vibration. If the actuator disengaged the clutch, the schematic diagram of a simplified model for the clutch control is in Figure 16.

The equation of motion for computing angular acceleration is rewritten as:

$$I_c\ddot{\theta}_w = nT_c - T_t \tag{44}$$

$$T_c = \mu_c N_c r_c \tag{45}$$

Where μ_c deputes the clutch coefficient of friction. In addition, I_c and T_t are introduced in (27)-(28). In the state space, angular acceleration, $\ddot{\theta}_w$ ($G_{(s)}$ in Figure 17) rewritten in (47):

$$x_2 = \dot{\theta}_w \tag{46}$$

$$\dot{x}_2 = \ddot{\theta}_w = \frac{nT_c}{I_c} - \frac{T_t}{I_c} \tag{47}$$

Where x_2 presents angular velocity. Since the shuffle, the output of the system is in the form of acceleration so it is considered the car acceleration as feedback which is compared with the driver-demanded acceleration. An I-type controller uses the difference between these two accelerations to build the control signal (See Figure 17).

The controller makes a supposition torque T_c which the restriction of clutch normal force N_c is predicted by it. By electronic control unit (ECU) command, the clutch actuator exerts this force on the clutch. If the transferred driveline torque exceeds N_c, the clutch slides, and consequently, the oscillation is dampened. The transfer functions are calculated as:

$$\frac{y}{u} = \frac{Kn}{Kn + SI_c} \tag{48}$$

$$\frac{y}{T_t} = -\frac{S}{Kn + SI_c} \tag{49}$$

and the root of the characteristic equation, S is:

$$S = -\frac{Kn}{I_c} \tag{50}$$

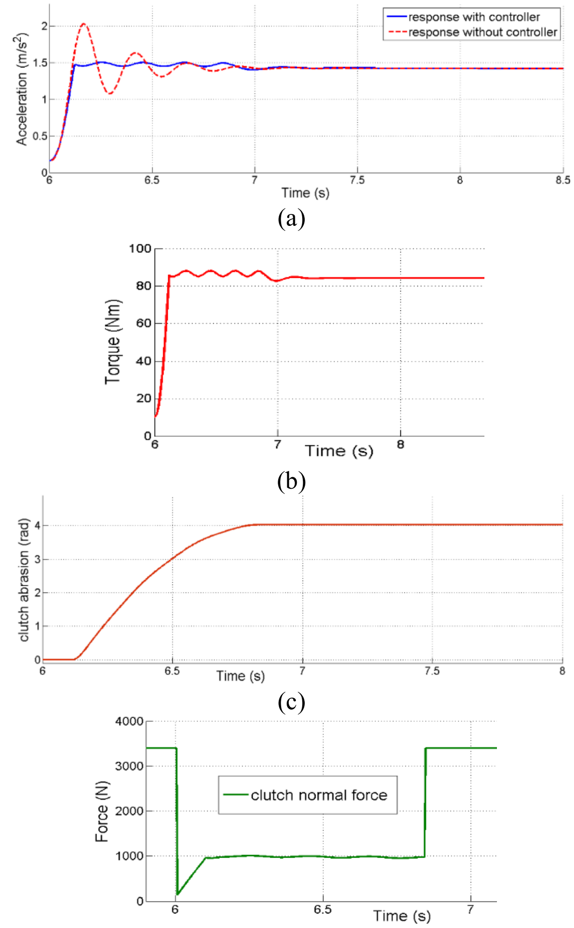

Figure 15: Response with and without pulse controller. (a): acceleration, (b): clutch torque, (c): abrasion between two surfaces of a clutch, and (d): clutch normal force variation.

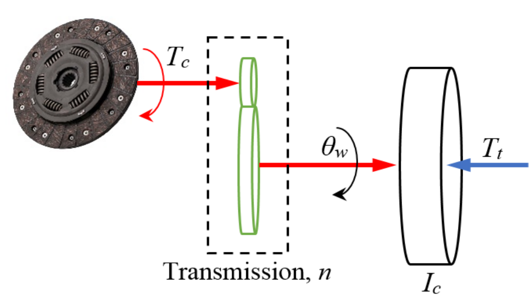

Figure 16: Simplified model for the clutch control

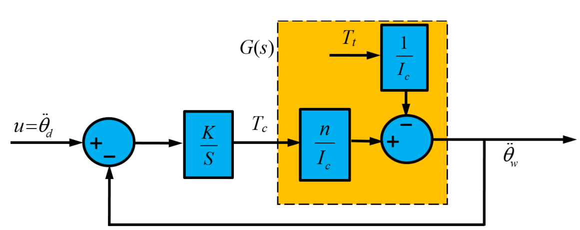

Figure 17: Block diagram of the vehicle driveline control.

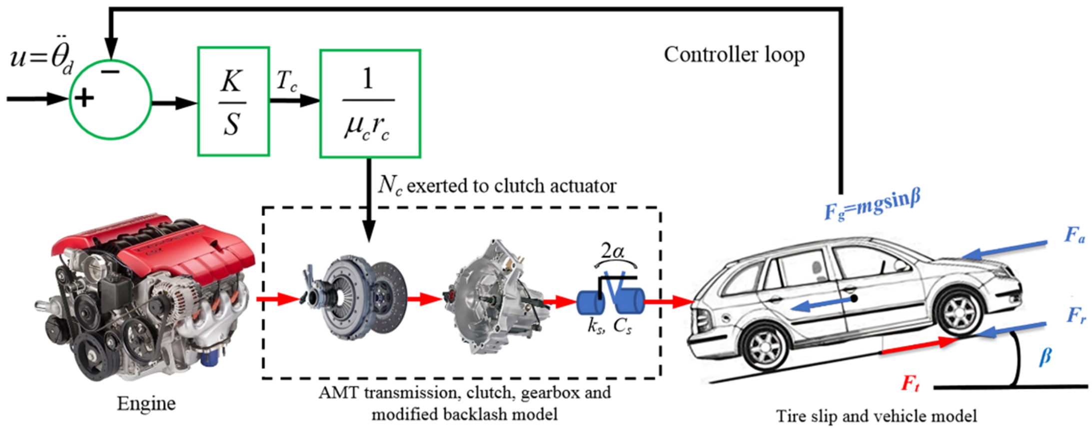

Figure 18: Clutch control loop.

From the positive gain K, S lies on the left-hand side from the real axis, thus the system is stable. After transient response, the output reaches to desired acceleration which is demanded by the driver. Finally, the complete control loop for longitudinal oscillation control is shown in Figure 18.

3.7. Controller action

The sampling time of the Volkswagen ECU is 0.01 seconds [21]. At this time by the speed sensor, ECU can compute vehicle acceleration. This is a time when the controller makes the controlling signal and sends it to the actuator. Also, the duration that the clutch can fully disengage is 0.1 seconds [27].

In testing conditions, in the sixth second, the tip-in scenario happens. In the sixth second, the ECU can sense the rapid change in the throttle position and activate the controller. The controller gets the error signal and computes the passing torque limitation. The response of the vehicle is provided in Figure 19. The gain K in this condition is 600.

4. Gain scheduling predictive controller

The effect of controller gain on clutch lifetime is examined in this section. The lifetime of a clutch is very imperative and it is essential to examine the clutch lifetime in designing the controller. The clutch slip is a main factor for the clutch lifetime. If the clutch slip increases, the clutch lifetime is decreased. For research, the clutch abrasion (e.g. Figure 20) is considered. Smaller abrasion means less clutch wear and more lifetime. In this section, the result for the variation of the gain will be represented here.

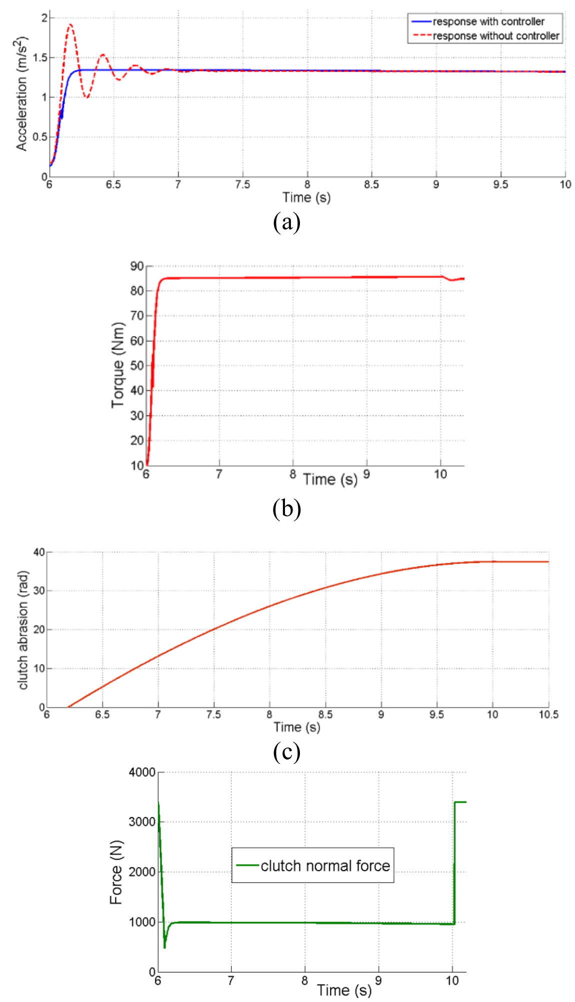

Figure 19: Response with and without the linear controller. (a): acceleration, (b): clutch torque, (c): abrasion between two surfaces of a clutch, and (d): clutch normal force variation.

4.1. Gain program

This research indicates that larger controller gains lead to an overshoot and for smaller controller gains, overshoot does not happen. Instead, the larger controller gains results in lower clutch slips (Figure 20).

To achieve lower oscillation with more clutch lifetime, during clutch control, the gain can be scheduled. Using a switching controller, at the start the gain will be held small to avoid the overshoot in controller response (this overshoot is named shunt). When the probability of shunt vibration is removed then the gain is quickly increased to lessen the wear of the clutch. In this work, it is found that the linear variation for the gain controller is appropriate. Thus, the gain controller is defined as:

$$\begin{cases} K = 600 & \text{for } t \le 0.3 \\ K = 600 + 600(t - 0.3) & \text{for } t > 0.3 \end{cases} \tag{51}$$

By trial and error, the number of 600 was found. The schematic diagram of the gain scheduling predictive controller is illustrated in Figure 21.

For the tip-in scenario, the results of this gain program are shown in Figure 22. By Comparing Figure 19c and Figure 22d, it is obvious that using this method leads to the clutch wear mostly diminished.

5. Conclusions

The idea of driveline vibration control with a dry clutch was studied in this work. First, a simulation package that has a comprehensive model including the clutch characteristics, a modified model for backlash, driveline shafts, and a tire full model was created and validated with experimental data. Then three approaches for shuffle and shunt control are considered: rule-based control, pulse control, and linear control. Comparing these controllers with each other (Figures 14,15, and 19) shows that rule-based and pulse controllers are easily implemented and low-cost. But relative to acceleration response, they have an oscillatory response and lower performance than the linear controller. Also, from a clutch abrasion viewpoint, the pulse controller has the best performance with the least wear and is the best choice for increasing clutch lifetime.

In the following, it was shown that a constant gain for a linear controller removes vibrations well but it causes the reduction of a clutch lifetime (Figure 20). Thus, a gain program was introduced to regulate the gain when the controller acts.

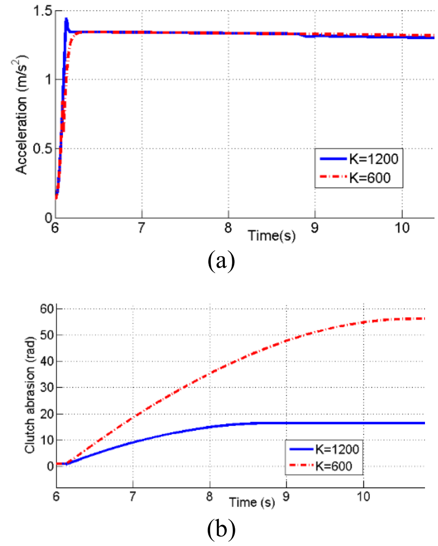

Figure 20: Vehicle response to the constant gain linear controller. (a): acceleration and (b): abrasion between two surfaces of a clutch.

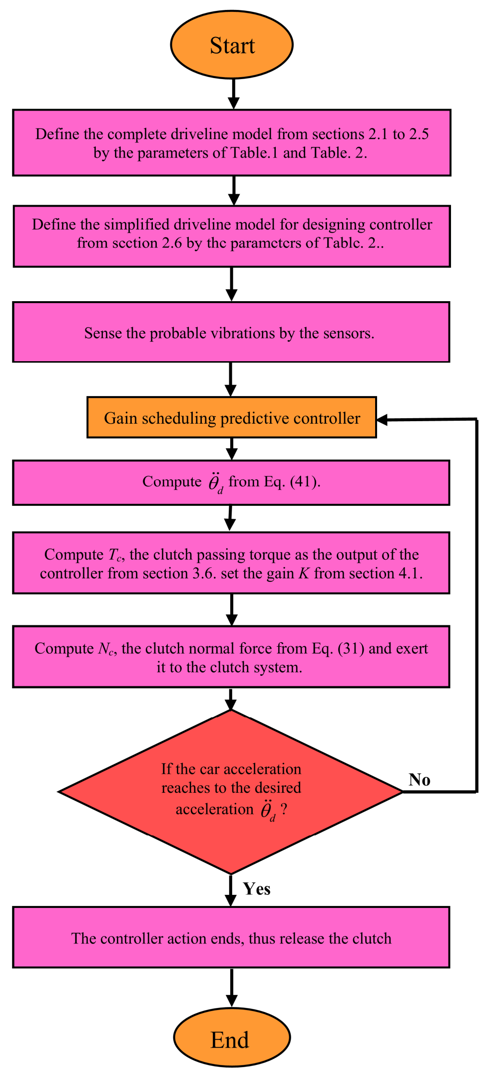

Figure 21: The controller Schematic diagram.

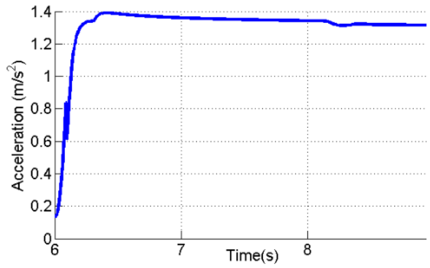

(a)

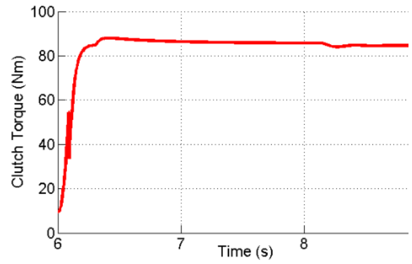

(b)

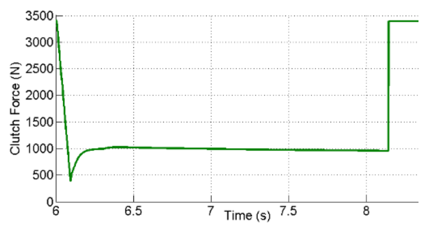

(c)

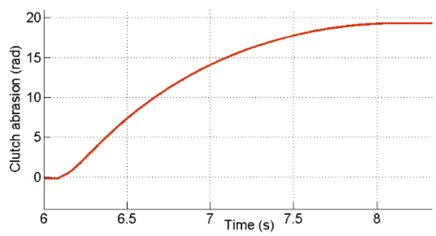

(d)

Figure 22: Vehicle response to gain scheduling linear controller. (a): acceleration, (b): clutch torque, (c): abrasion between two surfaces of a clutch, and (d): clutch normal force variation.

Table 4: Comparison of control methods

Method	Cost and implementation	Performance	Clutch wear
Rule-based control	Good	Moderate	Moderate
Pulse control	Good	Poor	Very good
Linear control	Fairly good	Good	Poor
Gain scheduling linear control	Fairly good	Good	Moderate

Simulations acknowledge the gain program control effectively decreases the clutch wear and increases clutch lifetime. Comparing Figure 19c with Figure 22d, it is concluded that the use of the gain scheduling program can reduce clutch wear by half. As a result, for all three cases, the controllers act successfully in eliminating the vehicle shunt and shuffle. These methods are compared with each other in Table 4. The benefits of this idea compared with the other methods of controlling the driveline longitudinal vibrations are lower cost, lower time for development in vehicles, and easy implementation, specifically in automobiles that have AMT.

Declaration of Conflicting Interests

The authors declared no potential conflicts of interest with respect to the research, authorship, and/or publication of this article.

References

[1] J. Masri, M. Amer, S. Salman, M. Ismail, and M. Elsisi, A survey of modern vehicle noise, vibration, and harshness: A state-of-the-art, Ain Shams Engineering Journal, p. 102957, 2024.

[2] N. A. Ngoc, V. H. Quan, and N. M. Tien, Research on the Impacts of Vibration and Noise on Drivers in Vehicles, in 2024 7th International Conference on Green Technology and Sustainable Development (GTSD), 2024: IEEE, pp. 489-493.

[3] H. Schmidt, K. Buettner, and G. Prokop, Methods for virtual validation of automotive powertrain systems in terms of vehicle drivability-A systematic literature review, IEEE Access, 2023.

[4] S. Kim, H. Lee, J. Kim, and G. Park, Online adaptive identification of clutch torque transmissibility for the drivability consistency of high-performance production vehicles, Control Engineering Practice, vol. 147, p. 105926, 2024.

[5] P. Gao, H. Li, H. Liu, and C. Xiang, An innovative torsional vibration absorber of vehicle powertrain system: Prototype design, performance test, and control experiment, Mechanics Based Design of Structures and Machines, vol. 51, no. 6, pp. 3434-3466, 2023.

[6] P. Reddy et al., Control-oriented modeling of a vehicle drivetrain for shuffle and clunk mitigation, SAE Technical Paper, 0148-7191, 2019.

[7] H. Chu, W. Shi, Y. Jiang, and B. Gao, Driveline Oscillation Damping for Hybrid Electric Vehicles Using Extended-State-Observer-Based

Compensator, Sustainability, vol. 15, no. 10, pp. 1-16, 2023.

[8] F. Barin, K. Heidari Shirazi, and H. M. Sedighi, Classification of transient vibration of passenger cars powertrain, Proceedings of the Institution of Mechanical Engineers, Part K: Journal of Multi-body Dynamics, p. 14644193231177866, 2023.

[9] H. Rahnejat, P. Johns-Rahnejat, N. Dolatabadi, and R. Rahmani, Multi-body dynamics in vehicle engineering, Proceedings of the Institution of Mechanical Engineers, Part K: Journal of Multi-body Dynamics, p. 14644193231181666, 2023.

[10] X. S. Xu, R. G. Dong, D. E. Welcome, C. Warren, T. W. McDowell, and J. Z. Wu, Vibrations transmitted from human hands to upper arm, shoulder, back, neck, and head, International journal of industrial ergonomics, vol. 62, pp. 1-12, 2017.

[11] A. Balluchi, L. Benvenuti, C. Lemma, P. Murrieri, and A. L. Sangiovanni-Vincentelli, Hybrid models of an automotive driveline, Tech. rep., PARADES, 2004.

[12] Q. Zhao, Study on Driveline Component Torsional Stiffness Effect on RWD Driveline Torsional Vibration Modes, in Proceedings of the FISITA 2012 World Automotive Congress, 2013: Springer, pp. 87-102.

[13] K. Togai and M. Platten, Input Torque Shaping for Driveline NVH Improvement and Torque Profile Approximation Problem with Combustion Pressure, in Proceedings of the FISITA 2012 World Automotive Congress, 2013: Springer, pp. 151-165.

[14] J. Fredriksson, H. Weiefors, and B. Egardt, Powertrain control for active damping of driveline oscillations, Vehicle System Dynamics, vol. 37, no. 5, pp. 359-376, 2002.

[15] D. Lefebvre, P. Chevrel, and S. Richard, An H-infinity-based control design methodology dedicated to the active control of vehicle longitudinal oscillations, Control Systems Technology, IEEE Transactions on, vol. 11, no. 6, pp. 948-956, 2003.

[16] H. Yonezawa, A. Yonezawa, T. Hatano, S. Hiramatsu, C. Nishidome, and I. Kajiwara, Active Reduction of Transient Driveline Oscillations with Fuzzy Update Timings of Control Input, in 2022 10th International Conference on Control, Mechatronics and Automation (ICCMA), 2022: IEEE, pp. 108-115.

[17] M. Pettersson and L. Nielsen, Diesel engine speed control with handling of driveline resonances, Control Engineering Practice, vol. 11, no. 3, pp. 319-328, 2003.

[18] E. Galvagno, D. Morina, A. Sorniotti, and M. Velardocchia, Drivability analysis of through-the-road-parallel hybrid vehicles, Meccanica, pp. 1-16, 2013.

[19] E. Galvagno, M. Velardocchia, and A. Vigliani, Drivability enhancement and transient emission reduction for a mild hybrid diesel–electric truck, International Journal of Powertrains, vol. 2, no. 2, pp. 262-291, 2013.

[20] Y. Qin et al., Noise and vibration suppression in hybrid electric vehicles: State of the art and challenges, Renewable and Sustainable Energy Reviews, vol. 124, p. 109782, 2020.

[21] Nicholas M. Northcote The modeling and control of an automotive drivetrain, Ms thesis, Department of mechanical engineering University of Stellenbosch April 2006.

[22] H. Chen, B. Gao, H. Chen, and B. Gao, Clutch disengagement timing control of AMT gear shift, Nonlinear Estimation and Control of Automotive Drivetrains, pp. 147-156, 2014.

[23] S. Lin, B. Li, M. Tang, and L. Wang, Precise and coordinated gearshift control for AMT gearshift system equipped with two linear actuators, Mechanics & Industry, vol. 25, p. 8, 2024.

[24] B. Mashadi and M. Badrykoohi, Driveline oscillation control by using a dry clutch system, Applied Mathematical Modelling, vol. 39, no. 21, pp. 6471-6490, 2015.

[25] F. Djemal, A. Ghorbel, O. Graja, M. Abdennadher, L. Walha, and M. Haddar, Vibration analysis of nonlinear powertrain model with randomly cracked teeth under acyclism operation, Journal of the Brazilian Society of Mechanical Sciences and Engineering, vol. 43, no. 9, p. 433, 2021.

[26] G. Naus, M. Beenakkers, R. Huisman, M. van de Molengraft, and M. Steinbuch, Robust control of a clutch system to prevent judder-induced driveline oscillations, Vehicle System Dynamics, vol. 48, no. 11, pp. 1379-1394, 2010.

[27] G. Lucente, M. Montanari, and C. Rossi, Modelling of an automated manual transmission system, Mechatronics, vol. 17, no. 2, pp. 73-91, 2007.

[28] A. Senatore, V. D'AGOSTINO, R. Di Giuda, and V. Petrone, Experimental investigation and neural network prediction of brakes and clutch material frictional behaviour considering the sliding acceleration influence, Tribology international, vol. 44, no. 10, pp. 1199-1207, 2011.

[29] R. Nouailletas, E. Mendes, and D. Koenig, Hybrid modeling and identification of dry friction systems, application to a clutch actuator, Control Engineering Practice, vol. 18, no. 8, pp. 904-917, 2010.

[30] D. A. Haessig Jr and B. Friedland, On the modeling and simulation of friction, 1991.

[31] H. Pacejka, Tire and vehicle dynamics. Elsevier, 2005.

[32] K. Jo, J. Kim, and M. Sunwoo, Real-Time Road-Slope Estimation Based on Integration of Onboard Sensors With GPS Using an IMMPDA Filter, Intelligent Transportation Systems, IEEE Transactions on, vol. 14, no. 4, pp. 1718-1732, 2013.

[33] H. Ohnishi, J. Ishii, M. Kayano, and H. Katayama, A study on road slope estimation for automatic transmission control, JSAE review, vol. 21, no. 2, pp. 235-240, 2000.

[34] Y. Sebsadji, S. Glaser, S. Mammar, and J. Dakhlallah, Road slope and vehicle dynamics estimation, in American Control Conference, 2008, 2008: IEEE, pp. 4603-4608.